Connectivity-based EEG-neurofeedback in VR: pipeline development and experimental validation

Cristiano Berhanu
cristiano.berhanu@tecnico.ulisboa.pt

Instituto Superior Técnico, Lisboa, Portugal

October 2019

Abstract

Neurofeedback (NFB) is a process through which individuals, by receiving information about a feature of their neural activity, may learn, through training, to discriminate and self-regulate that feature of interest. Introduced over forty years ago, it has since been used mostly in clinical research and practice related to neurological and psychiatric conditions. The greater focus of research on clinical efficiency has, however, not helped elucidate through what mechanisms learning occurs, and it has not been investigated how different brain features may be optimally trained. The emergence of views on brain function stemming from findings that connectivity between remote brain regions is fundamental to healthy brain function, that this connectivity has a dynamical nature on various time-scales, and that local dysfunction often carries a network effect, has increased the interest in using functional connectivity as a feature for neurofeedback training. In this work, functional connectivity algorithms were developed and integrated in an open-source electroencephalography (EEG) processing software (OpenViBE), and a pipeline was developed for an EEG-based neurofeedback experiment in virtual reality (VR). Finally, a pilot study was conducted to assess the efficacy of training, using the newly developed EEG-NFB system. Two groups of subjects underwent four training sessions, using: i) a previously well-established feature, the amplitude of the individual upper alpha and ii) the newly proposed and implemented feature, the weighted node degree of the functional connectivity. Results show a tendency for increase of the upper alpha and functional connectivity along training. Furthermore, alpha training appears to affect functional connectivity in a significant way. This study provides evidence of the possibility to target functional connectivity with NFB, and of the efficacy of VR as a stimulus delivery mechanism.
Keywords: Neurofeedback, Functional Connectivity, Virtual Reality,

1. Introduction

Neurofeedback (NFB) is the process of gaining greater awareness/control of brain activity by providing the subject external sensory or behavioural feedback based on the current state of his/her brain activity [1]. The feedback usually consists of a real time display of neural activity, which may be acquired through electroencephalography (EEG), magnetoencephalography (MEG), functional magnetic resonance imaging (fMRI) or functional near infrared spectroscopy (fNIRS) [2]. This allows selective manipulation and regulation of a specific pattern of neural activity (such as the amplitude of the alpha band). Joe Kamiya was the first to observe, in 1969, that some subjects had the apparent ability (after some training) to discern whether they were in a state with high alpha power ("alpha state") and to enter this state on command [3]. This heightened control of brain activity has been, over the last decades, explored from the therapeutic point of view, and currently neurofeedback treatment is available in specialty clinics for an array of disorders and impairments, such as attention deficit and hyperactivity disorder (ADHD), epilepsy, depression, anxiety, Parkinson's disease, alcoholism and post traumatic stress disorder, being also used for performance improvement [2]. However, although current literature generally evaluates neurofeedback as a valid means of regional brain activity modulation, its therapeutic efficacy in disease states is still in its early stages, with many studies suffering from small sample sizes, methodological limitations (such as inadequate blinding and/or absence of sham control treatment), and contradictory findings [4]. These shortcomings may be attributable to an insufficient understanding of the neurobiological mechanisms that modulate regional brain activity and translate it into cognitive and motor functions [5]; but NFB, by making neural activity an independent variable (which may be modulated through training) might actually help answering the question, by allowing observation of the effect of specific

changes in neural activity patterns on behaviour. When it comes to how the feedback is presented, no clear guidelines currently exist, although some findings suggest better results for auditory rather than visual feedback [6], and virtual reality (VR) as an improvement from simple on screen visual feedback [7, 8], providing greater immersion and comfort and reduced boredom [9]. NFB experiments with EEG usually aim for training of specific frequency band modulation (eg. alpha training, beta training) or modulation of a ratio between two bands (eg. alpha/theta training), although recently training of different brain activity patterns has been attempted.

Historically, brain mapping has aimed mainly at functional segregation and localization of brain function. As the early phrenologic idea that specific complex actions and emotions could be attributed to single cortical areas was refuted, it was realized that a cortical area is specialized for some aspects of perceptual or motor processing, a specialization that is segregated within the cortex. Thus, a single function may involve several specialized areas, and the brain may be seen as a complex network of interacting subsystems [10, 11]. As research progressively unveiled the workings of several segregated brain areas, the question of how functional integration mediates their union came within grasp, and over the last decade overwhelming interest arose in this area. This integration may be characterized in terms of functional connectivity (FC), which may be defined as the statistical dependencies between remote neurophysiological events [10]. Even in resting-state (in the absence of any given task) FC exhibits meaningful spontaneous variations accessible through neuroimaging techniques [12]. FC is generally considered to happen through (or be accompanied by) inter-regional synchronization of neuronal oscillations, which may happen over a wide range of spatial and temporal scales [13]. For a practical identification and monitoring of the temporal evolution of large scale networks involving distant brain regions, EEG is one of the available techniques, providing enough temporal resolution to capture the changes of functional connectivity as cognitive events manifest themselves, and a low cost of operation. However, effectively measuring synchronization is not straightforward, with obstacles arising due to EEG's inherent low spatial resolution, and the fact that recorded signals can hardly be said to consist of oscillations at discrete frequencies, rendering the concept of synchronization inadequate [13]. A plethora of different FC measures exists for EEG based on the ideas of coherence and phase-locking, each aiming to handle some of the intrinsic limitations of the EEG signal in an *ad-hoc* fashion, often times unmotivated by a proper mathematical background, rather consisting of empirical addenda to previously used methods in order to address interpretational difficulties [14]. Disruption of FC for specific networks is associated with several diseases [15], and FC has been found to be modulated during learning tasks as well as to help predict performance of these tasks [16]. Recent findings establish a causal link between FC modulation through NFB training and behavioural effects, such as symptom reduction in patients of Autistic Spectrum Disorders and motor function improvement in stroke patients [17, 18]. Interestingly, one recent study showed increased functional connectivity within a specific brain network as a consequence of alpha/theta NF training [19].

In this work, algorithms for measuring real time FC in EEG data have been implemented and an EEG-based NFB system in VR has been developed and tested on two groups of healthy volunteers, targeting the upper alpha frequency band, and aiming to test, for one, the possibility of increasing a measure of FC and its behavioural effects (i.e. working memory assessment), and for the other, the possibility of increasing the relative amplitude of the upper alpha and its behavioural effects.

2. Measuring Functional Connectivity in EEG

In this section a brief overview is presented of the implemented algorithms. This choice of algorithms present a trade-off between estimated quality of the algorithms, as assessed through reported performance, the extent of their use in the available literature, ease of implementation, low computational cost and availability in open source software (for validation) [20, 21, 11, 22].

Coherence and Coherency

For two signals $x(t)$ and $y(t)$, we may say they are correlated if we can predict the variations of one as a function of the other. This can be simply estimated by the Pearson-correlation coefficient:

$$R = max_\tau \frac{cov(x(t), y(t+\tau))}{\sigma_x \sigma_{y_\tau}} \tag{1}$$

where $cov(x(t), y(t+\tau))$ is the covariance between signal $x(t)$ and signal $y(t)$ shifted by time τ, σ_x is the standard deviation of $x(t)$ and σ_{y_τ} is the standard deviation of $y(t+\tau)$. High absolute values of R indicate that x reproduces the variations of y, with a time lag τ (R has values between -1 to 1). If we are interested in finding out this relationship at a specific frequency f, we can band pass the signal narrowly around f and then estimate R, which may then be referred to as coherence [23]. A signal x can, however, be represented in the frequency domain:

$$X(f,t) = A(f,t)e^{i\phi(f,t)} \tag{2}$$

with $A(f,t)$ the amplitude and $\phi(f,t)$ the phase of the signal (the angle between the real and the imaginary part of x). Hence coherence between $x(t)$ and $y(t)$ can be formulated as:

$$C(f,t) = \frac{S_{xy}(f,t)}{S_{xx}(f,t)S_{yy}(f,t)} = \frac{X(f,t)\overline{Y(f,t)}}{\sqrt{X^2(f,t)Y^2(f,t)}} \tag{3}$$

where $S_{xx}(f,t)$ and $S_{yy}(f,t)$ are the power spectral densities of $x(t)$ and $y(t)$, and $S_{xy}(f,t)$ is their cross-spectral density (all may be obtained by Fourier transforming the corresponding correlation function) [24]. This last formula is often referred to as *coherency*, which has values in the complex plane whereas *coherence* would be the absolute value of coherency. Coherence has been often used in connectivity analysis.

Phase Locking Value

For a signal representation such as in eq. 2, the temporal structure of the signal is contained in the phase ϕ, and in a simple case of a time delay between signals $x(t)$ and $y(t)$ at frequency f, a corresponding phase shift exists, that is linearly related to f. Knowing this, we might be interested in excluding the amplitude from a synchronization analysis, and focus solely on the phase. By observing instantaneous phase differences

$$\Phi(f,t) = |n\phi_x(f,t) - m\phi_y(f,t)| \qquad m,n \in \mathbb{Z} \tag{4}$$

it is possible to determine a limited time window where this difference is approximately constant, i.e. where *phase-locking* occurs. The phase-locking value (PLV) was thus created for sole quantification of phase relationships between signals. This is possible through calculation of the instantaneous phase of the signal for each instant t through a wavelet transform (or equivalently, with a Hilbert transform [25]). It may be expressed as:

$$plv_{xy}(f,\tau) = \frac{1}{|\tau|}\sum_{t\in\tau} e^{i(\phi_x(f,t)-\phi_y(f,t))} \tag{5}$$

where $|\tau|$ represents the number of time points in the trial.

Imaginary Part of Coherency

Considering that volume conduction from the sources of electrical activity to the electrodes in the scalp may be considered instantaneous for the frequencies of interest in EEG [26], then we would obtain a zero phase shift between two signals with potentials arising from the same source, whereas for actual functional connectivity there would be a shift in phase, corresponding to the time period for an active source to synchronize with another one in a different region. Hence, the portion of coherency due to volume conduction effects will always have a real value (since for a coherency of $C = Ae^{i\phi}$, if the phase ϕ is zero then C is located in the real axis of the complex plane) while real connectivity would be complex with, generally, a non-negligible imaginary part (except for when a true interaction produces a phase lag between signals of a multiple of 180 degrees). This notion was described by Nolte et al [20], and motivated the use of the imaginary part of coherency (ImC) for functional connectivity measurement:

$$ImC_{xy}(f,\tau) = \frac{\Im\Big(S_{xy}(f,\tau)\Big)}{\sqrt{S_{xx}(f,\tau)S_{yy}(f,\tau)}} \tag{6}$$

where $\Im(.)$ denotes the imaginary part.

Phase Slope Index

Besides estimating which regions are interconnected, determining the direction of information flow is of great interest. A robust approach for this estimation was developed by Nolte et al that used as basis the imaginary part of the coherency [21]. The main idea is as follows: if there is a real interaction between two sources x and y, the flow of information from one to the other will take some time. Assuming that different waves travel at similar speed, then the phase difference ($\Delta\phi(f) = \phi_x(f) - \phi_y(f)$) between the signals of each source will increase linearly with the frequency, and as such a positive slope of the phase spectrum is expected. As an example, consider the simple case where there is only a time delay between the two signals:

$$y(t) = x(t - t_0) \tag{7}$$

In the frequency domain, this becomes:

$$Y(f) = e^{-i2\pi f t_0}X(f) \tag{8}$$

Thus the cross spectrum S_{xy} between the two signals will be proportional to $e^{i2\pi f t_0} = e^{i\Phi(f)}$. If the slope of $\Phi(f)$ is positive, x causes y, and vice-versa. By selecting a frequency window and estimating the slope, the further it deviates from zero, the greater the evidence of a causal relationship between the two signals. The phase slope index can then be defined as:

$$PSI_{xy}(f,\tau) = \Im\Big(\sum_{f\epsilon\ F} C^*_{xy}(f,\tau)C_{xy}(f+\delta f,\tau)\Big) \tag{9}$$

where: C_{xy} is the coherency, δf is the frequency resolution and F is the set of frequencies over which to compute the slope. How the above expression corresponds to a weighted sum of the slopes is best understood considering the following derivation, obtained through Euler's formula:

$$\begin{aligned}&\Im\Big(C^*_{xy}(f_1,\tau)C_{xy}(f_2,\tau)\Big) = \\ &\Big|C^*_{xy}(f_1,\tau)\Big|\,|C_{xy}(f_2,\tau)|\,sin(\Phi(f_2)-\Phi(f_1))\end{aligned} \tag{10}$$

Since for smooth phase spectra (i.e. small $\Delta\Phi$ between adjacent frequencies) we may approximate $sin(\Delta\Phi) \approx \Delta\Phi$, then it becomes clear the above expression consists of a weighted sum of the slopes. Furthermore, by taking the imaginary part, it will be insensitive to instantaneous interactions (one could also see that if there is no delay between two signals, the slope of the phase spectrum would be zero).

weighted Phase Lag Index

The imaginary part of coherency has some bias when identifying real interactions between brain regions, since it will be maximal for phase differences of 90 degrees between two signals (since the coherency is purely imaginary), and decreases to zero as the phase differences approach 0 or 180 degrees (since the coherency becomes purely real). To address this problem a new connectivity metric, the phase lag index, was created [11]. It assesses to what extent positive or negative phase differences are equiprobable, irrespective of their magnitude. In other words, if there is a consistent, non-zero phase lag between two signals then there is connectivity. The weighted phase lag index, introduced a few years later, simply weights the magnitudes of the phase differences, which helps clarify situations where small perturbation turn a phase lead to a phase lag [22]. Assessing if a phase difference between to signals is positive or negative can generally be done by considering the sign of the imaginary part of coherency, $sgn(\Im(C_{xy}))$ (which yields -1 if negative or 1 if positive), which, to be sure, is equal to the sign of the imaginary part of only cross-spectrum, since the denominator of the coherency is always real. The phase lag index is then defined as:

$$PLI_{xy} = \left| \frac{1}{|\tau|} \sum_{t\in\tau} sgn(\Im(S_{xy})) \right| \tag{11}$$

where the instantaneous cross-spectrum is obtained through a Hilbert or wavelet transform, and averaging is performed over the whole epoch. The weighted phase lag index, on the other hand, is defined as:

$$wPLI_{xy} = \frac{\left| \sum\limits_{t\in\tau} |\Im(S_{xy})|\, sgn(\Im(S_{xy})) \right|}{\sum\limits_{t\in\tau} |\Im(S_{xy})|} = \frac{\left| \sum\limits_{t\in\tau} \Im(S_{xy}) \right|}{\sum\limits_{t\in\tau} |\Im(S_{xy})|} \tag{12}$$

Thus there is weighting of the phase leads and lags, which rids the estimation of noisy phase differences very close to zero, and the normalization leads to an estimate that is independent of the magnitude of the phase difference (unlike the imaginary part of coherency). Furthermore, by excluding the amplitudes of each individual signal from the normalization process, this measure is less susceptible to noise and more sensitive to real connectivity.

3. Algorithm Testing

the MATLAB toolbox Fieldtrip was used to generate connectivity data and Fieldtrip's connectivity algorithms were used as a reference for the obtained results [27]. EEG Data was generated with the use of the function *ft_connectivitysimulation*, which allows the simulation of channel-level time-series data with a specified connectivity structure. For testing on OpenVibe, this data was exported as a *.gdf* file. Each test was created in order to address some of the most common issues which arise when interpreting functional connectivity findings in EEG. Each test is detailed below.

Common reference

Data for two channels with a common reference was simulated on Fieldtrip. Two scenarios were created, one with a real coupling between the signals, and another with no coupling. Note that if for two channels the reference electrode is the same (which is true in a majority of EEG recordings), then any activity detected in the reference electrode will be present in both channels' recordings, increasing their correlation with one another (without any delay), and connectivity between the two channels may be incorrectly inferred. Observing the results in figure 1 (top left section), it is clear that the magnitude squared coherence presents common reference artifacts. With the ImC and wPLI, this effect disappears. The PSI algorithm, although able to correctly distinguish between real connectivity and common signal, has a much lower sensitivity to real connectivity. Note that real coupling corresponding to a phase delay of 0 mod 180 degrees would remain unidentified but for the magnitude squared coherence, since the other algorithms extract only the imaginary part of the cross-spectrum.

Volume Conduction

Data for the sources of electric activity was generated through an auto-regressive model, with 50 channels and a diagonal co-variance matrix, with large values for the 16th and 35th source (to simulate different signal to noise ratios present in real data). A connectivity analysis of this data may be seen in figure 1 (bottom left section), which shows the obtained connectivity matrices for all sensor pairs. It becomes clear that both the MSCoh and the PLV show hypersensitivity to instantaneous interactions through volume conduction (seen as the high connectivity values along the diagonal). All other algorithms identify no regions of high connec-

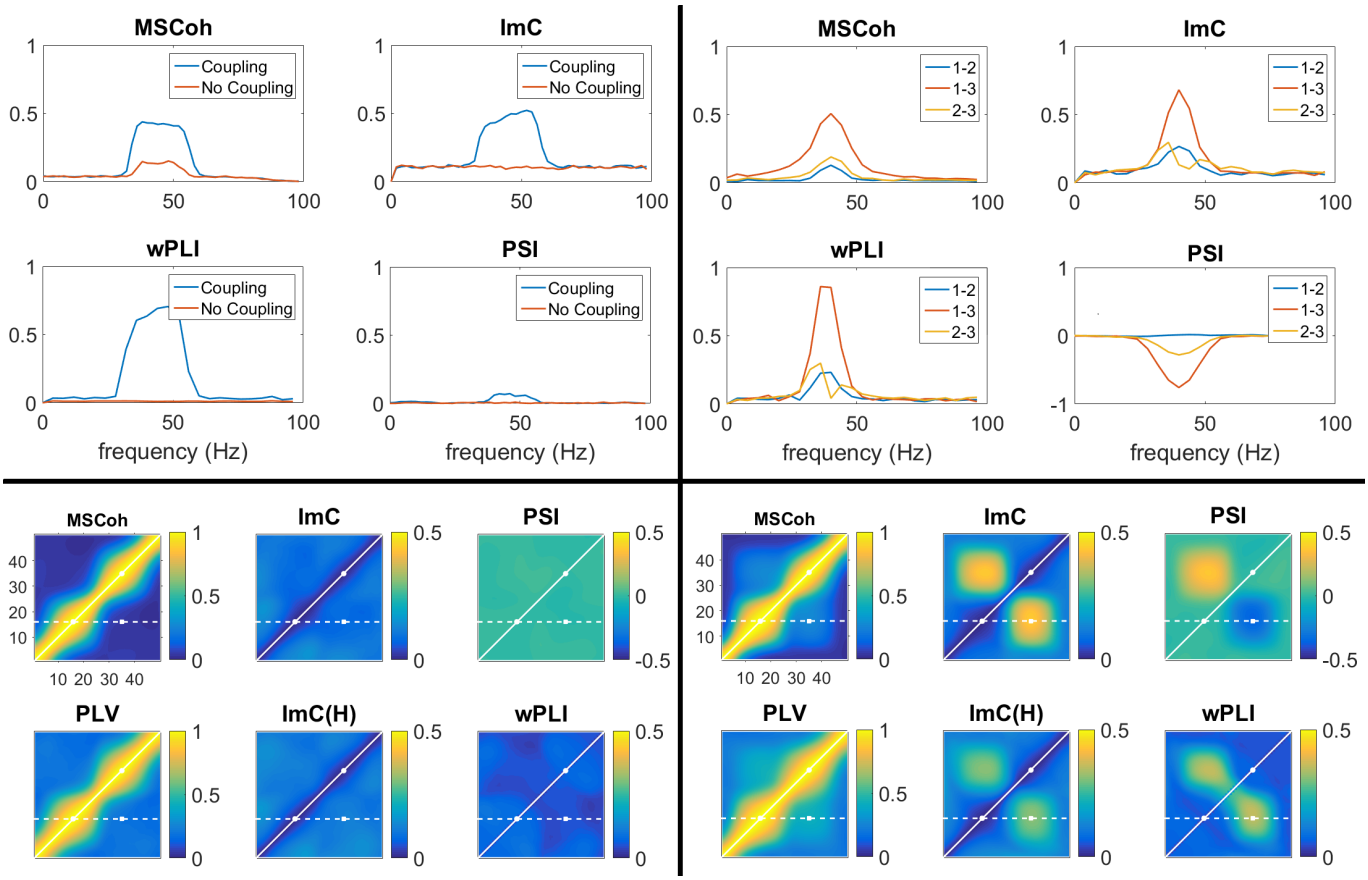

Figure 1: Top left: Connectivity values for common reference data with (blue) and without coupling (red).Top right: Pairwise connectivity values between 3 channels where channel 3 influences channels 1 and 2 with different time lags. Bottom left: Case with no real connectivity. Each connectivity matrix presents the connectivity values pairwise between all sensors. Bottom right: Real connectivity between channels 16 and 35. Note: MSCoh = Magnitude Squared Coherence, ImC = Imaginary part of Coherency, PSI = Phase Slope Index, wPLI = weighted Phase Lag Index, ImC(H) = imaginary part of coherency through the Hilbert transform (opposed to the Welch method).

tivity, although there is some background artifactual connectivity. To simulate real connectivity, the 16th and 35th source were connected with a non-zero time lag. We can see in figure 1 (bottom right section) that the ImC (both implementations), the wPLI and the PSI all correctly identify the connection. With MSCoh and PLV, the real connectivity is overshadowed by the volume conduction effects.

Common Input

In order to determine what difficulties arise when a source (channel 3) acts as a driver on two others (channels 1 and 2), connectivity data for 3 channels was simulated in Fieldtrip with an autoregressive model. The driver (channel 3) was connected to one of the sources at lag 1 (channel 1) and to the other at lag 2 (channel 2). The results are displayed in figure 1 in the top right section. Since the third source is connected to source 1 and 2 with different time lags, it is harder to identify the connection between sources 1 and 2 as spurious, which only the phase slope index accomplishes. Furthermore, since the time lag between sources 3 and 2 is larger, it is harder to identify their connection. Note that since with the PSI we are evaluating the information flow from channels 1 and 2 to channel 3 the value obtained is negative, indicating that information flow is in the opposite direction.

4. Methods

The experiments were conducted in the NeuroLab room of the Evolutionary Systems and Biomedical Engineering Lab (LaSEEB), a research lab of the Institute of Systems and Robotics (ISR). The signals were recorded using the EEG amplifier LiveAmp (Brain Products GmbH, Germany) through the open source software OpenViBE (Inria Rennes, France) with a 500Hz sampling frequency from ActiCap's system of 32ch (32 channels) active electrodes. The ground was placed at the forehead

and the reference over the left mastoid (channel TP9). Circuit impedance was kept below $25k\Omega$. For the feedback presentation, Oculus Rift Virtual reality glasses were used (Oculus VR, United States).

This study aimed at determining the effects of training the power of the individual upper alpha band and functional connectivity (also for the individual upper alpha). Frequencies of interest were adjusted to each subject because of reported inter-individual differences [28]. The RAUA was obtained from the electrode Cz, by taking the average power in the upper alpha band and dividing by the average of the power over all frequencies $(4-30Hz)$, as defined by [29]:

$$RAUA = \frac{\sum_{k=\frac{IAF}{\Delta f}}^{\frac{HTF}{\Delta f}} X(k)}{HTF - IAF} / \frac{\sum_{k=\frac{4}{\Delta f}}^{\frac{30}{\Delta f}} X(k)}{30 - 4} \tag{13}$$

where HTF and IAF are the higher transition frequency and the individual alpha frequency, Δf is the frequency resolution and $X(k)$ is the magnitude of the spectrum of the signal fom Cz at frequency bin k. Functional connectivity was obtained considering the weighted node degree (WND) of the imaginary part of Coherency for electrode Cz. Here, each electrode is considered a node or vertex of a weighted graph. Each electrode has edges connecting it to all others; edges whose weight is the connectivity between the two electrodes they join (given by the imaginary part of coherency). WND is obtained for one electrode by summing all pairwise connectivities between that electrode and all others:

$$k_i = \sum_{j \in E} ImC_{ij} \tag{14}$$

where ImC_{ij} is the imaginary part of the coherency between electrodes i and j and E is the set of all electrodes. The weighted node degree can thus be interpreted as the absolute importance of a node in the network. Since this analysis is done in sensor space, not much physical meaning may be ascribed to the WND value, in terms of brain regions or networks involved. The imaginary part of coherency was chosen, among the available algorithms, because it presented stable results in simulations (see section 3); it has, to a greater extent than other recent approaches, been used in real data and particularly in neurofeedback studies [17, 30, 15]. Its implementation is also widely available in open-source software, guaranteeing the offline processing of the signals from this study.

Participants

A total of 8 healthy subjects took part in the experiment. Most participants were students or researchers. Participation was voluntary and not compensated monetarily. There were no exclusion criteria, nevertheless no participant suffered serious health problems, psychiatric or psychological disorders. Participants were asked to complete self-assessment health-related questionnaires (including 36-item Short Form Survey (SF-36) and Hospital Anxiety and Depression Scale (HADS)). Subjects were semi-randomly distributed between two groups (with similar to male/female ratio in each group). The alpha group consisted of 4 subjects (2 males and 2 female, with ages in the range 34 ± 12), and so did the functional connectivity group (3 males and 1 female, with ages in the range 27.5 ± 5.5)

Session Design

Each training session was divided into 5 sets composed of 3 blocks each, which in turn consisted of 2 1-minute trials. Between each trial there were pauses of at least 10-15 seconds. Total training time was around 37 minutes. The paradigm for the training was slightly different each session. For the first session, the subject was asked to increase the size of a rotating sphere of particles; for the second session, the subject was asked to increase the rotation speed of the sphere of particles; for the third session, the subject was asked to try and enter the sphere of particles. For the fourth session, a mix of all paradigms was used. Baselines were acquired before and after each session. After each session, participants were asked to fill two questionnaires (simulator sickness and NASA-TLX), concerning their opinions of the session. Another questionnaire, regarding the VR experience, was filled after the last session. There were in total four sessions, executed on consecutive days. Before the first session and after the last session the N-back test was performed for most of the participants, in order to assess working memory.

Assessing training effect

The indices from [6] were used to assess the training effect. The first three ($Intra1$, $Intra2$ and $IntraS$) capture variations of the feedback parameter over each session, while the last three ($Inter1$, $Inter2$ and $InterS$) account for variations over the different sessions. The indices are:

$$Intra1 = \frac{\sum_{i=1}^{nsessions} \sum_{j=1}^{nsets} \frac{\bar{set}_{i,j} - \bar{set}_{i,1}}{\bar{set}_{i,1}}}{nsessions(nsets - 1)} \tag{15}$$

$$Intra2 = \frac{\sum_{i=1}^{nsessions} \frac{\bar{set}_{i,5} - \bar{set}_{i,1}}{set_{i,1}}}{nsessions} \tag{16}$$

$$IntraS = \frac{\sum_{i=1}^{nsessions} m_i}{nsessions} \tag{17}$$

$$Inter1 = \frac{(\bar{S}_4 + \bar{S}_5) - (\bar{S}_1 + \bar{S}_2)}{\bar{S}_1 + \bar{S}_2} \tag{18}$$

$$Inter2 = \frac{(\bar{set}_{4,4} + \bar{set}_{4,5}) - (\bar{set}_{1,1} + \bar{set}_{1,2})}{\bar{set}_{1,1} + \bar{set}_{1,2}} \quad (19)$$

$$InterS = m \quad (20)$$

where $\bar{set}_{i,j}$ stands for the mean of the set j of session i, $nsessions$ is the total number of sessions, $nsets$ is the total number of sets and m_i represents the slope of session i Working memory was assessed by the N-back task (2-back and 3-back). Unfortunately this was not performed for all the subjects (5 subjects performed this test).

5. Results

In this section, the results of the neurofeedback experiment are presented. First the targeted measure is analysed for each group (5), then non-targeted frequency bands and other measures are investigated to assess specificity of training (5). A brief presentation of the cognitive performance before and after the training is then given (5). Finally, an overview of the participants answers to the questionnaires is presented, together with any correlations with the results of the training.

Effect along training

All results are presented for the targeted electrode, Cz. We can see in figure 2 the evolution of the relative alpha amplitude (left 4 columns) and of the functional connectivity (right 4 columns) along the 5 sets of each session. For the alpha group, we see an upwards tendency, excepting subject A4, and specially marked in the first session. For the connectivity group, the fluctuations are less monotone and harder to evaluate visually. However, it appears that for all subjects of both groups the baseline acquired after the last session presents a higher value of the feedback parameter that the baseline acquired before the first session.

The bottom left of figure 2 presents for each session and for each subject the mean RAUA (left) and the mean WND (right). Only subject A3 shows a substantial increase from the first to the subsequent sessions in the alpha group. In the connectivity group subjects FC2 and FC4 show a clear increase in their WND over sessions. The bottom right of figure 2 presents for each set and for each subject the mean over all sessions. All subjects in the alpha group show a slight increase during the sessions, with the exception of subject A3, which shows a non-linear decrease. For the connectivity group there is no clear increase, with the connectivity values oscillating wildly, and peaking halfway through the session.

Specificity of training

In order to determine if the results obtained are specific to the targeted frequency bands, the feedback measure (RAUA or WND, depending on the group) was calculated for other frequency bands. Assessment of the progress was done using the indices described in section 4. Positive values for the indices means an increase of the feedback measure over the different sets (*Intra*) or over different sessions (*Inter*). Figure 3 shows the distribution for all participants of the indices for the targeted frequency band (upper alpha) and for the theta band (4-7 Hz) and beta band (HTF-30 Hz, recall that HTF is the upper bound of the upper alpha band). It is clear from the left part of figure 3 that the upper alpha band shows the greatest increase during the session. The theta band shows great variance, with positive values for some participants and very negative ones for others. Functional connectivity also appears to increase more significantly for the alpha band, with small positive variations for the other bands. From the right part of figure 3 there appears to be no considerable increase for any of the frequency bands. The theta band, however, shows a great variance among subjects. Functional connectivity appears to increase more significantly for the upper alpha over the different sessions.

In order to further assess specificity, the feedback measure of each group was calculated for the opposite group. Figure 4 represents the distribution of the training indices across all individuals. The upper alpha appears to be affected only by alpha training, since the connectivity group shows virtually no alpha variation. The functional connectivity of the alpha group shows, however, an increase comparable to the functional connectivity of the connectivity group for all indices.

Working Memory

The N-back test was conducted for 5 subjects only (out of the 8): 3 from the connectivity group and 2 from the alpha group. Figure 5 presents the distribution of the results of the N-back test for all participants. There appears to be a slight increase in accuracy, more evident in the distractor groups, i.e. when letters are not targets and the participant should not react to them. The reaction times also appear to increase slightly for the N-3 part of the task. Individual results are presently assessed. There appears to be no significant patterns of increase or decrease of the reaction times. Regarding accuracy, there is also no clear indication of a better performance after the neurofeedback training. Subject A3, A4, FC3 increase their performance in the distractor group of both the N-2 and N-3 parts, with FC3 obtaining a better accuracy in all parts of the task. FC2 increased performance only in the target groups. Only subject FC4 decreased performance in several parts of the task.

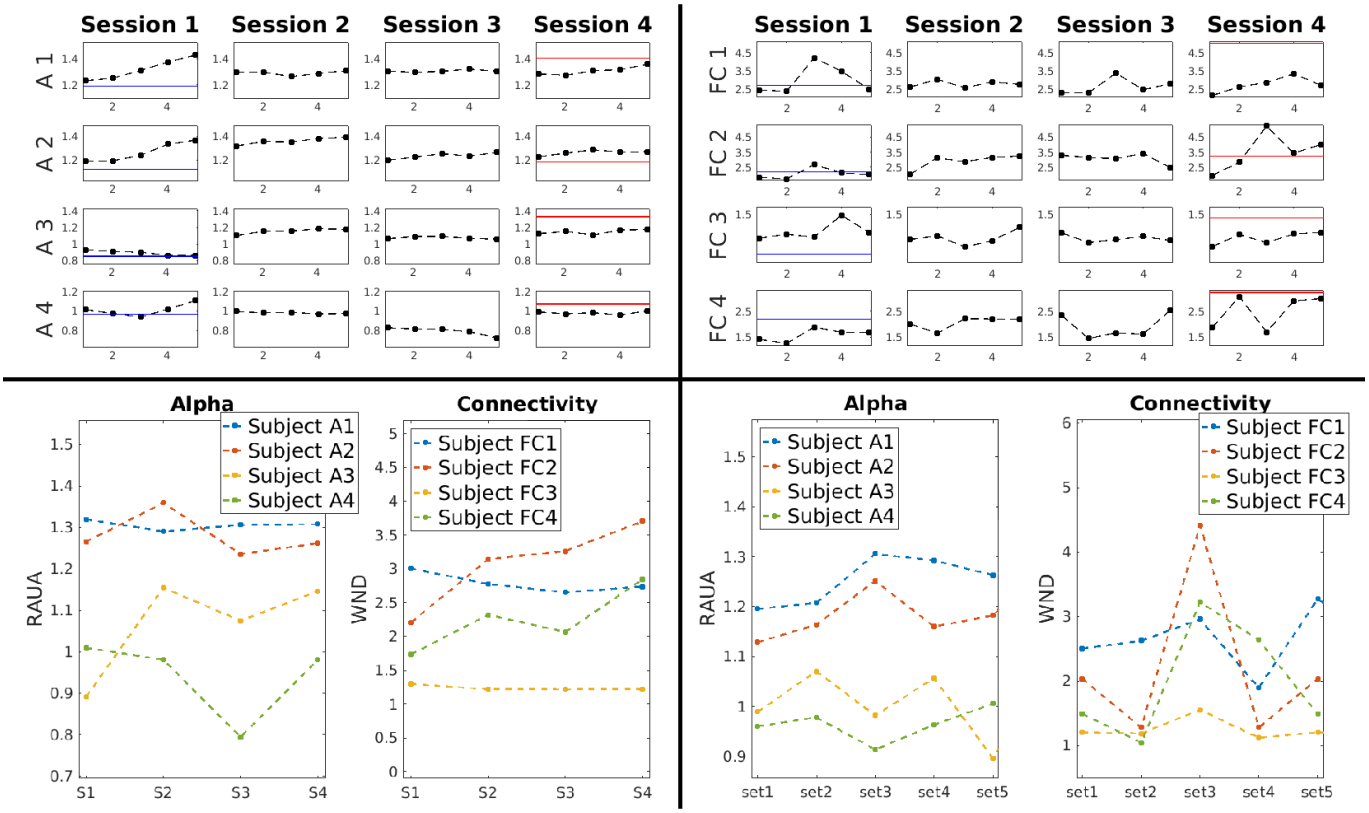

Figure 2: Top: Progression of the RAUA (Subjects A1 to A4) and WND (subjects FC1 to FC4) along each session. Each data point represents the mean of the set. The blue lines represent the value of the baseline previous to the first training session and the red lines the baseline posterior to the last training session. Bottom left: Individual subject's evolution of the RAUA (left) and connectivity (right) at channel Cz across sessions. Bottom right: Individual subject's evolution of the RAUA (left) and connectivity (right) at channel Cz across sets.

6. Discussion

Implemented algorithms

The implemented algorithms, ImC, wPLI, PSI, ciPLV, showed consistency with other available implementations (namely, the ones from the Fieldtrip toolbox). Metrics using the Welch method seem to have performed slightly better than metrics using the Hilbert transform (note differences between two implementations of ImC in the bottom of figure 1). This might be because when using the Welch approach, a complex signal is obtained from each segment, while for the Hilbert approach the instantaneous phase is obtained using the whole trial; furthermore, the phase being instantaneous, it is more subject to noise.

Weighted Node Degree

A brain network can be equated to a graph, where each independent region is a node and the edges connecting each pair of nodes are as strong as the functional connectivity between each pair. One common procedure to assess the overall importance of a node in a network is to compute the weighted node degree, by computing the target node's connectivity with all other brain regions in the network. In this work the overall importance of the Cz channel was determined, in the network composed by all 32 channels. This was done in an exploratory manner; no immediate physical meaning can be ascribed to the strength of the node Cz in this network. In fact, all network analysis in sensor space are severely flawed in that attribution of brain regions to different channels is not possible.

Effect along training

A training effect during sessions was observed for both groups, as shown by the overall tendency for increase of the feedback measure, which may be seen in the plots of figure 2, but also through the learning indices, which are positive for the great majority of subjects (figure 3, left part). Between sessions no effect is apparent for the alpha group, although the connectivity group shows some increase (right of figure 3). Alpha neurofeedback training has been widely conducted, and results have been reported both within and across sessions. Long-

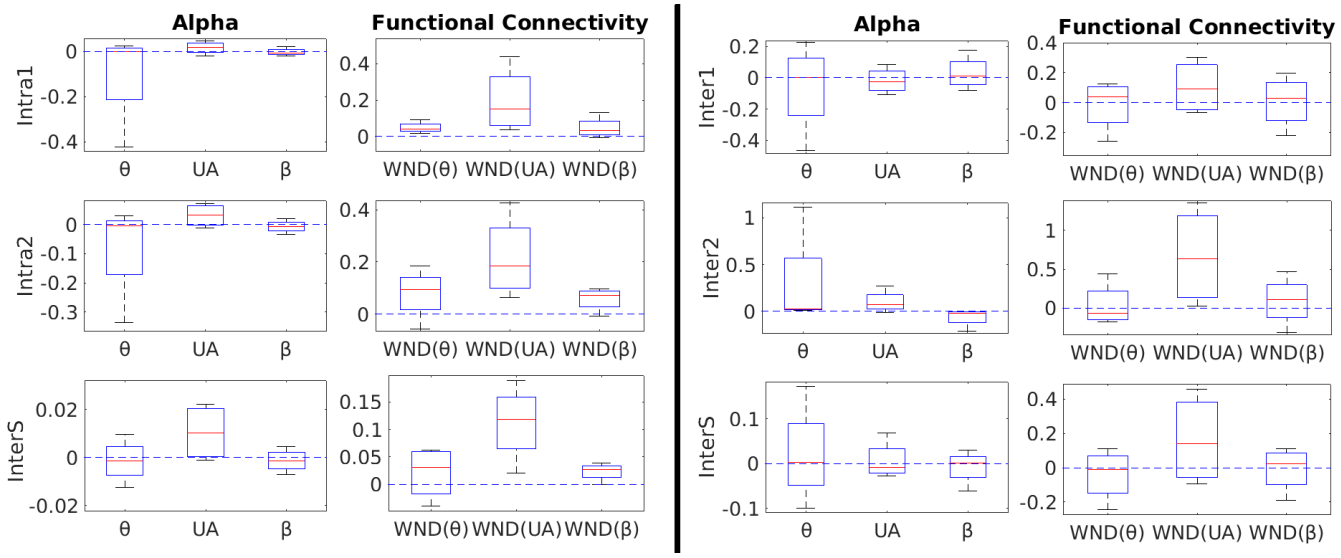

Figure 3: Distribution of the training indices for assessment of changes along and across sessions of all subjects for different frequency bands. UA is the upper alpha, the frequency band targeted during training

term effect on the upper alpha band has been described, as well as increasing, cumulative effects over subsequent sessions. Reports on single session changes of the RAUA are conflicting, with some authors finding significant increases of the feedback measure and others not. Regarding functional connectivity, few studies have been conducted, but progress has been reported within as well as across sessions [30, 31]. The performance obtained across sessions might not have been significant enough due to the low number of sessions (four), which was lower than recommended (eight to ten) for higher chances of success [32]. Regarding the RAUA calculation, not only does the choice of reference affect the spectral estimation, but also removal of noise components (through ICA), even in non-targeted frequencies, will affect the normalization process (eq. 13). The effects on functional connectivity will be even greater: the choice of reference has been shown to directly affect connectivity estimation, and depending on the metric and the nature of the noise, the effect of noise removal has rather unpredictable consequences [33, 34].

Specificity of Training

Specificity of the neurofeedback was assessed by calculating the feedback measure for frequency bands of no interest, but also by calculating the feedback measure of the opposite group. This later approach allowed, beyond assessing specificity of training, insight into the effect of alpha training on functional connectivity and vice-versa. Comparison between these different conditions was done through the learning indices (section 4), as seen in figures 3-4. Within session, the relative spectral amplitude appears to be modulated mainly in the frequency band of interest (upper alpha), with negligible effects in the beta band. Reports, however, suggest non-specificity of training and, in, particular, a negative correlation between alpha and theta band amplitude, which was not found here [28, 32]. Regarding the WND, within sessions the effect appears to be mainly in the upper alpha frequencies, but there is also an effect in the theta band to a smaller degree, and even a slight increase in the beta band. There has been, to the author's knowledge, only one connectivity-based neurofeedback study assessing band specificity of learning (target frequencies 8-12Hz), which found that, indeed, progress was somewhat restricted to the band of interest (with some spilling to neighbouring frequencies) [30]. Through the computation, for each group, of the feedback measure of the opposite group, it appears evident that upper alpha connectivity training has no effect on the amplitude of the upper alpha band, which coincides with previously reported findings [30]. On the other hand, the values of functional connectivity for the alpha group vary quite a lot, which is in agreement with previous reports that alpha neurofeedback training has repercussions at the network level, and so this effect on functional connectivity may be caused by the alpha amplitude changes evoked by the neurofeedback training [19].

Working Memory

There appears to be no significant changes in the accuracy and reaction times of the N-back test, which

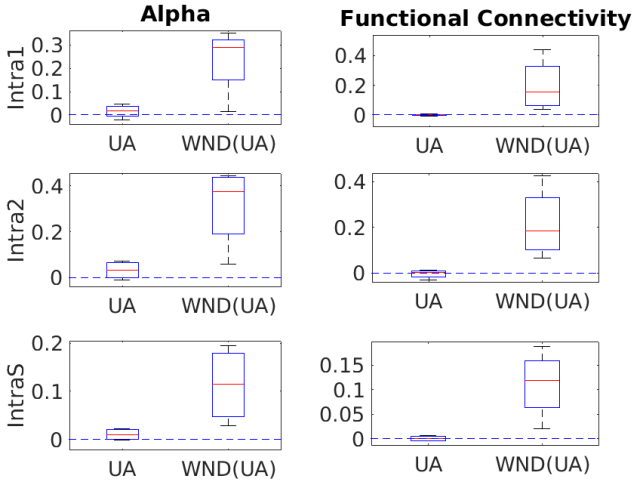

Figure 4: Distribution of the training indices for assessment of changes along each session of all subjects for the trained measure and the measured trained by the other group.

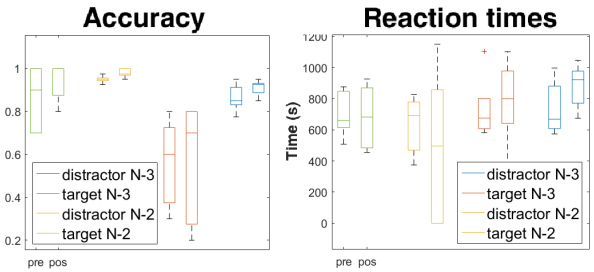

Figure 5: Distribution of the N-back results for all participants. Left: accuracy in identifying real instances (target) and not identifying wrong ones (distractor) for N=2 and N=3. Right: reaction times in identifying real instances (target) and identifying wrong ones (distractor) for N=2 and N=3. Note that if there are no false positives the reaction time is zero.

may also be due to the very small sample size. That being said, the accuracy, taken over all the subjects, shows an increasing tendency, being higher after the training sessions. The literature suggests that the number of sessions necessary to evoke cognitive changes should be higher [32]. On the other hand, the simple fact that the same task was performed twice means that changes in performance may come from increased experience with the task. Without a control group there is no way to confirm that the neurofeedback training caused any observable changes.

7. Conclusions

This work attempted to sketch from beginning to end a connectivity-based neurofeedback experiment in VR. As the path was threaded upon, progressive awareness of the challenges made it clear that each step was due more attention and careful planning than was available to spare. In any case, a small number of functional connectivity algorithms was implemented and the experiment pipeline was successfully developed and deployed on a small group of voluntaries (N=8). The implemented algorithms were consistent with currently available solutions, and dealt well with common artifacts caused by, among others, volume conduction and common referencing. The participants were divided into two groups, one for alpha training and the other for connectivity training. There was no clear evidence of an ability to self-regulate either the amplitude of the upper alpha or an overall measure of functional connectivity, neither were there any cognitive (working memory) enhancements; which were in any case unlikely, given the small sample size and the small number of training sessions. There was, however, a proclivity for alpha increase within each session. Functional connectivity also showed an increase both within sessions as well as across sessions. The effects happened mostly in the frequencies of interest (individual upper alpha), although there was some effect in neighbouring frequency bands. There was indication that neurofeedback performance might correlate negatively with perceived mental demand and hard work, which could be informative on the mechanisms through which neurofeedback learning occurs.

Acknowledgements

Thank you to supervisors Patrícia Figueiredo, Agostinho Rosa and Athanasios Vourvopoulos.

References

[1] Danielle S. Bassett and Ankit N. Khambhati. A network engineering perspective on probing and perturbing cognition with neurofeedback. *Annals of the New York Academy of Sciences*, 1396(1):126–143, April 2017.

[2] Robert T. Thibault, Michael Lifshitz, and Amir Raz. The self-regulating brain and neurofeedback: Experimental science and clinical promise. *Cortex*, 74:247–261, January 2016.

[3] Jon A. Frederick. Psychophysics of EEG alpha state discrimination. *Consciousness and Cognition*, 21(3):1345–1354, September 2012.

[4] Nicholas Lofthouse, L. Eugene Arnold, Sarah Hersch, Elizabeth Hurt, and Roger DeBeus. A review of neurofeedback treatment for pediatric ADHD. *Journal of Attention Disorders*, 16(5):351–372, November 2011.

[5] Sharon Niv. Clinical efficacy and potential mechanisms of neurofeedback. *Personality and Individual Di erences*, 54(6):676–686, April 2013.

[6] Teresa Bucho. Comparison of auditory and visual modalities for eeg-neurofeedback. *Master's thesis, Instituto Superior Tecnico, Lisbon, Portugal*, October 2018.

[7] Michelle Wang and Denise Reid. Virtual reality in pediatric neurorehabilitation: Attention deficit hyperactivity disorder, autism and cerebral palsy. *Neuroepidemiology*, 36(1):2–18, 2011.

[8] John Gruzelier, Atsuko Inoue, Roger Smart, Anthony Steed, and Tony Steffert. Acting performance and flow state enhanced with sensory-motor rhythm neurofeedback comparing ecologically valid immersive VR and training screen scenarios. *Neuroscience Letters*, 480(2):112–116, August 2010.

[9] Ilkka Kosunen, Mikko Salminen, Simo Järvelä, Antti Ruonala, Niklas Ravaja, and Giulio Jacucci. Relaworld: Neuroadaptive and immersive virtual reality meditation system. In *Proceedings of the 21st International Conference on Intelligent User Interfaces*, IUI '16, pages 208–217, New York, NY, USA, 2016. ACM.

[10] Karl J. Friston. Functional and effective connectivity: A review. *Brain Connectivity*, 1(1):13–36, January 2011.

[11] Cornelis J. Stam, Guido Nolte, and Andreas Daffertshofer. Phase lag index: Assessment of functional connectivity from multi channel EEG and MEG with diminished bias from common sources. *Human Brain Mapping*, 28(11):1178–1193, 2007.

[12] Maria Giulia Preti, Thomas AW Bolton, and Dimitri Van De Ville. The dynamic functional connectome: State-of-the-art and perspectives. *NeuroImage*, 160:41–54, October 2017.

[13] Francisco Varela, Jean-Philippe Lachaux, Eugenio Rodriguez, and Jacques Martinerie. The brainweb: Phase synchronization and large-scale integration. *Nature Reviews Neuroscience*, 2(4):229–239, April 2001.

[14] André M. Bastos and Jan-Mathijs Schoffelen. A tutorial review of functional connectivity analysis methods and their interpretational pitfalls. *Frontiers in Systems Neuroscience*, 9, January 2016.

[15] Adrian G. Guggisberg, Susanne M. Honma, Anne M. Findlay, Sarang S. Dalal, Heidi E. Kirsch, Mitchel S. Berger, and Srikantan S. Nagarajan. Mapping functional connectivity in patients with brain lesions. *Annals of Neurology*, 63(2):193–203, February 2008.

[16] C. M. Lewis, A. Baldassarre, G. Committeri, G. L. Romani, and M. Corbetta. Learning sculpts the spontaneous activity of the resting human brain. *Proceedings of the National Academy of Sciences*, 106(41):17558–17563, October 2009.

[17] Anaïs Mottaz, Tiffany Corbet, Naz Doganci, Cécile Magnin, Pierre Nicolo, Armin Schnider, and Adrian G. Guggisberg. Modulating functional connectivity after stroke with neurofeedback: Effect on motor deficits in a controlled cross-over study. *NeuroImage: Clinical*, 20:336–346, 2018.

[18] Robert Coben, Morgan Middlebrooks, Howard Lightstone, and Madeleine Corbell. Four channel multivariate coherence training: Development and evidence in support of a new form of neurofeedback. *Frontiers in Neuroscience*, 12, October 2018.

[19] Claudio Imperatori, Giacomo Della Marca, Noemi Amoroso, Giulia Maestoso, Enrico Maria Valenti, Chiara Massullo, Giuseppe Alessio Carbone, Anna Contardi, and Benedetto Farina. Alpha/theta neurofeedback increases mentalization and default mode network connectivity in a non-clinical sample. *Brain Topography*, 30(6):822–831, September 2017.

[20] Guido Nolte, Ou Bai, Lewis Wheaton, Zoltan Mari, Sherry Vorbach, and Mark Hallett. Identifying true brain interaction from EEG data using the imaginary part of coherency. *Clinical Neurophysiology*, 115(10):2292–2307, October 2004.

[21] Guido Nolte, Andreas Ziehe, Vadim V. Nikulin, Alois Schlögl, Nicole Krämer, Tom Brismar, and Klaus-Robert Müller. Robustly estimating the flow direction of information in complex physical systems. *Physical Review Letters*, 100(23), June 2008.

[22] Martin Vinck, Robert Oostenveld, Marijn van Wingerden, Franscesco Battaglia, and Cyriel M.A. Pennartz. An improved index of phase-synchronization for electrophysiological data in the presence of volume-conduction, noise and sample-size bias. *NeuroImage*, 55(4):1548–1565, April 2011.

[23] William A. Gardner. A unifying view of coherence in signal processing. *Signal Processing*, 29(2):113–140, November 1992.

[24] Julius S. Bendat and Allan G. Piersol. *Random Data: Analysis and Measurement Procedures*. Wiley, 1971.

[25] Michel Le Van Quyen, Jack Foucher, Jean-Philippe Lachaux, Eugenio Rodriguez, Antoine Lutz, Jacques Martinerie, and Francisco J. Varela. Comparison of hilbert transform and wavelet methods for the analysis of neuronal synchrony. *Journal of Neuroscience Methods*, 111(2):83–98, September 2001.

[26] Robert Plonsey and Dennis B. Heppner. Considerations of quasi-stationarity in electrophysiological systems. *The Bulletin of Mathematical Biophysics*, 29(4):657–664, December 1967.

[27] Robert Oostenveld, Pascal Fries, Eric Maris, and Jan-Mathijs Schoffelen. FieldTrip: Open source software for advanced analysis of MEG, EEG, and invasive electrophysiological data. *Computational Intelligence and Neuroscience*, 2011:1–9, 2011.

[28] Wolfgang Klimesch. EEG alpha and theta oscillations reflect cognitive and memory performance: a review and analysis. *Brain Research Reviews*, 29(2-3):169–195, April 1999.

[29] Feng Wan, Wenya Nan, Mang I. Vai, and Agostinho Rosa. Resting alpha activity predicts learning ability in alpha neurofeedback. *Frontiers in Human Neuroscience*, 8, July 2014.

[30] Anais Mottaz, Marco Solcà, Cécile Magnin, Tiffany Corbet, Armin Schnider, and Adrian G. Guggisberg. Neurofeedback training of alpha-band coherence enhances motor performance. *Clinical Neurophysiology*, 126(9):1754–1760, September 2015.

[31] Diljit Singh Kajal, Christoph Braun, Jürgen Mellinger, Matthew D. Sacchet, Sergio Ruiz, Eberhard Fetz, Niels Birbaumer, and Ranganatha Sitaram. Learned control of inter-hemispheric connectivity: Effects on bimanual motor performance. *Human Brain Mapping*, 38(9):4353–4369, June 2017.

[32] John H. Gruzelier. EEG-neurofeedback for optimising performance. III: A review of methodological and theoretical considerations. *Neuroscience & Biobehavioral Reviews*, 44:159–182, July 2014.

[33] Dror Cohen and Naotsugu Tsuchiya. The effect of common signals on power, coherence and granger causality: Theoretical review, simulations, and empirical analysis of fruit fly LFPs data. *Frontiers in Systems Neuroscience*, 12, July 2018.

[34] Yunzhi Huang, Junpeng Zhang, Yuan Cui, Gang Yang, Ling He, Qi Liu, and Guangfu Yin. How different EEG references influence sensor level functional connectivity graphs. *Frontiers in Neuroscience*, 11, July 2017.